# Manipulation of Islands on Freely Suspended Smectic Films and Bubbles Using Optical Tweezers

A. Pattanaporkratana[1], C. S. Park[2], J. E. Maclennan[3], and N. A. Clark[4]

Ferroelectric Liquid Crystal Materials Research Center, Department of Physics,
University of Colorado, Boulder, CO 80309, USA
[1]e-mail: pattanap@Colorado.EDU; [2]e-mail: cpark@bly.Colorado.EDU;
[3]e-mail: jem@ Colorado.EDU; [4]e-mail: clarkn@ Colorado.EDU

*Abstract*

*Smectic liquid crystals can be made to form freely suspended films and bubbles, locally quantized in thickness by an integral number N of smectic layers, on which islands, circular regions of greater thickness than the surrounding film area, can be generated. Here we demonstrate that such islands can be manipulated using optical tweezers. We have investigated experimentally and theoretically the optical trapping forces on islands with radii in the range* $1 < R < 100$ *µm and thickness* $N \sim 300$ *layers on background films and bubbles of* $N_f \sim 50$ *layers. With the trapping laser beam focused to a spot size small compared to the diameter of an island, the trapping force is found to be maximized when the edge of the island passes through the center of the beam, as predicted. The optical tweezer system will be used to study the static and dynamic interactions between islands.*

## I. Introduction

Smectic liquid crystals (LCs) are known to form stable freely suspended films, similar to soap films, when they are stretched over a solid frame [1]. Such films have been widely studied since Young et al. demonstrated quantization of thickness in units of smectic molecular layers and showed that molecular organization and director fluctuations could be observed and studied systematically in films as thin as two smectic layers [2]. Figure 1 shows reflected light photomicrographs of typical smectic films, illustrating the quantized nature of the film thickness: the layer number N is always integral, with only discrete changes in thickness occurring at places generically referred to as "layer steps". Such layer steps are edge dislocations in the smectic layering and can be viewed as a collection of interacting 1 dimensional (1D) interfaces in the 2D space of the film surface. Thickness changes and particularly islands, which are disk-shaped thicker regions of the film, are readily visualized because the reflected intensity (and for thicker films the reflected color) depends strongly on film thickness.

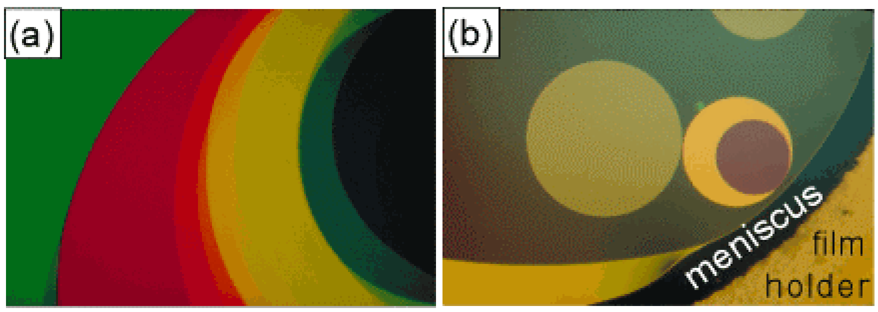


**Figure 1: Layer steps and islands on smectic A films 3 mm in diameter photographed in reflection soon after the films were created. The local film thickness is always an integral number of smectic layers $N_f$, one layer typically being about 30 Å thick. (a) Regions of different thickness, bounded by layer steps, show characteristic** interference colors**. (b) Islands are quite mobile and appear to float on the film. This image includes part of the film holder (at lower right) and shows the dark Plateau border (meniscus) along the film boundary.**

Film-forming smectics can also form stable bubbles, tethered on an inflating needle [3-6]. Tethered bubbles are of great interest for the study of the collective static and dynamic behavior of layer steps because the bubble geometry affords a much weaker coupling of layer steps to the bulk material contained in the bounding Plateau border than does the flat film geometry. By virtue of its shape, a bubble tethered on a needle of diameter r small compared to the bubble radius $R_b$ is characterized by a very large ratio of area to meniscus length $\lambda \sim R_b^2/r$, relative to that of a planar film of radius $R_f$, for which $\lambda \sim R_f$. When $\lambda$ is large, the morphology and evolution of layer steps is dominated by their mutual interaction, rather than by interactions, including the exchange of material, with the edge of the film.

Optical tweezers are widely used for trapping small objects that have a higher index of refraction than the surrounding medium [7,8]. In the case of a laser beam traveling through air, the integrated electrostatic energy is lowered if a dielectric material, such as liquid crystal, is introduced into the beam path. This effect would cause any LC material near the edge of a non-uniform laser to be attracted toward the center of the beam, where the optical fields are largest. We have applied this principle to the study of layer steps in freely suspended smectics, demonstrating that islands can be trapped and manipulated with optical tweezers.

## II. Experimental

We have used two liquid crystal materials, 8CB (BDH, $X \xleftrightarrow{21.5^oC} SmA \xleftrightarrow{33.5^oC} N \xleftrightarrow{40.5^oC} I$) and the chiral mixture MX8068 (Displaytech, Inc., $X \xleftrightarrow{-22^oC} SmC^* \xleftrightarrow{60.5^oC} SmA^* \xleftrightarrow{78^oC} N^* \xleftrightarrow{80.5^oC} I$), all experiments being performed at room temperature. The islands were observed using a reflected light microscope with infinity-corrected optics, allowing us to bring in the tweezing laser using a beam splitter placed just above the objective lens (see Figure 2). We used an Argon ion laser with wavelength $\lambda_0$ = 514.5 nm and power P ~ 250 mW. The laser beam, normally incident on the film's surface, was tightly focused by the objective. Images of the islands were obtained using a digital video camera.

Islands were studied on planar freely suspended films as well as on spherical bubbles. The flat films were 6 mm and the bubbles 10 mm in diameter, with the latter tethered on a needle 1 mm in diameter. Although islands sometimes form spontaneously while creating fresh films and bubbles, additional islands can be generated by rapidly flowing air over the film (bubble) surface. This induces shear flow in the film (bubble), which tears any excess material on the film (bubble) into small pieces. These fragments become islands, adopting a circular perimeter because of line tension. Experimentally, we find that we can generate more, smaller islands on bubbles in this way than we can on films. This is because the bigger $\lambda$ ratio in the bubble geometry enables much larger in-plane dynamic stress. Alternatively, islands can be created by shrinking the bubbles. The layer structure of an island is sketched in Figure 3.

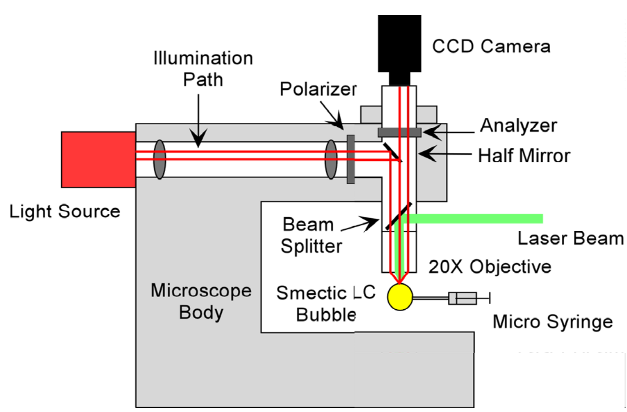


**Figure 2: Experimental setup for observation and optical trapping of islands on smectic films and bubbles. Bubbles are inflated from LC material covering the tip of a hypodermic needle by slowly injecting air through a micro syringe.**

**Figure 3: Profile of a 6-layer island on a 3-layer smectic film. The additional smectic layers defining the island are thought to be encapsulated within the film, as indicated.**

Bubbles present a unique opportunity for studying smectic islands in an environment where their behavior is hardly affected by the bounding meniscus. On freely suspended films, on the other hand, the island growth dynamics which is mediated by the flow of material on and off the film, is strongly dependent on the proximity of the boundary [9].

## III. Results and Discussion

We have successfully trapped islands on both freely suspended films and bubbles. Focusing the laser beam to a 10 μm spot (using a 20X objective lens) produced forces sufficient to trap islands with radii R in the range 1 ~ 100 $\mu$m. Trapping was confirmed by translating the film (bubble) and observing that, while other islands moved along with the film, the trapped island remained fixed in the laser beam. The trapping forces appeared to be of the same order in films and bubbles. Figure 4 shows a typical sequence of images of a trapped island in a moving film.

In 8CB films (smectic A at room temperature), we were able to induce coalescence of two islands by tweezing one island toward the other, as shown in Figure 5. We were not able to do this with films of MX8068 (smectic C* at room temperature), however, implying the existence of strong, short-range repulsive forces between islands of this material.

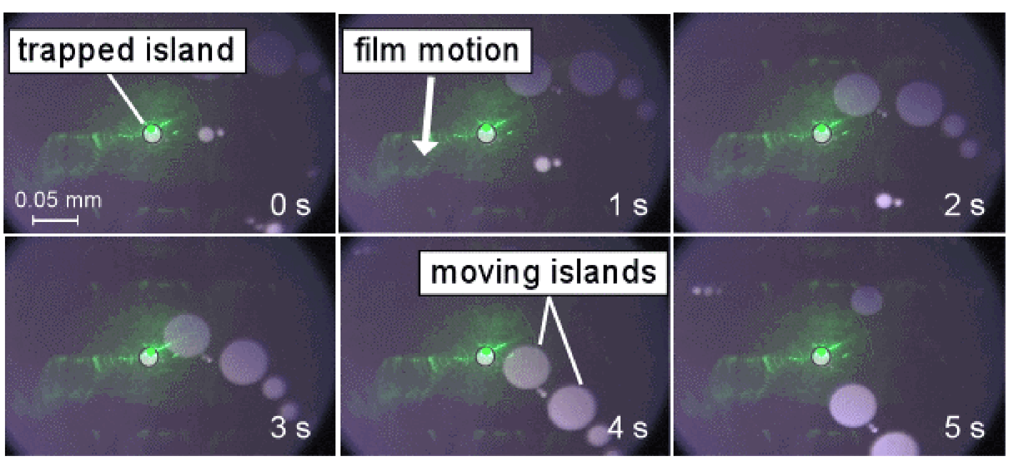


**Figure 4: Optically trapped island (circled) in a moving film of MX8068. The laser beam is seen as a bright green dot near the edge of the trapped island. The elapsed time between frames is 1 second.**

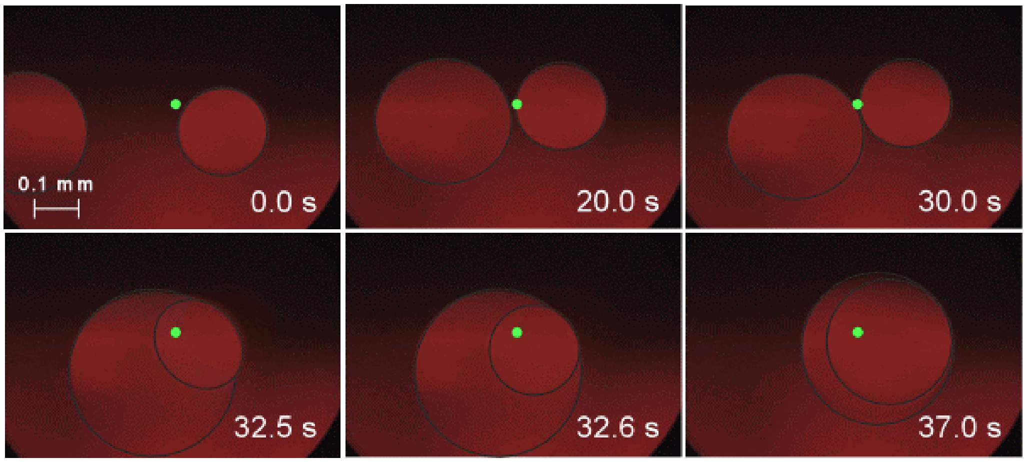


**Figure 5: Manipulation of islands on an 8CB film. First, the laser, indicated by the green dot, is used to trap the island on the right. A second island is then brought close to the trapped island by translating the entire film (to the right). When the two islands are maneuvered close enough together, they coalesce. The edges of the islands have been highlighted here for clarity.**

### *1. Theoretical Calculation of Optical Trapping Force*

We estimate the optical trapping forces on a LC island by considering the electromagnetic energy stored in a film/island system due to the optical field. The film is taken to be in the x-y plane, with the laser beam propagating along the z direction. Assuming a laser with radial Gaussian intensity profile, the change in energy due to the presence of LC in the beam path is given by

$$\begin{aligned}\delta U &= \frac{1}{2}\int(\vec{D}\cdot\vec{E}_{LC}-\vec{D}\cdot\vec{E}_{air})\,d^3x \\ &= -\frac{2P}{\pi c}\left(\frac{\kappa-1}{\kappa}\right)\int\frac{1}{w(z)^2}e^{-2\frac{x^2+y^2}{w(z)^2}}\,dx\,dy\,dz \qquad (1)\end{aligned}$$

where $P$ is the laser power, $c$ the speed of light, and $\kappa$ the dielectric constant of the liquid crystal. The laser beam width is described by $w(z)=w_0\sqrt{1+(z/z_0)^2}$ , where $z_0=\pi n w_0^2/\lambda_0$, $w_0$ the minimum waist of the laser, $n$ the index of refraction of the surrounding medium (we take $n\sim 1$ for air), and $\lambda_0$ the wavelength of the laser in the air. The integral in Eq. (1) is performed over the entire volume of the LC, assuming a film of thickness d, and an island of thickness h and radius R.

The dependence of the optical trapping force on island location is found by evaluating $-\vec{\nabla}\delta U$. The forces along the beam direction turn out to be negligible compared to those transverse to it. The radial trapping force F(ρ), as a function of island displacement from the center of the beam, is plotted for various island thicknesses and radii in Figure 6. When the center of the island wanders or is displaced from the beam center, the laser provides a restoring force, bringing the island back to the lowest energy, centered position. Figure 6 confirms that this force is greatest when the edge of the island finds itself at the center of the beam. This is to be expected since the discontinuity in film thickness at the island edge causes a huge lateral gradient in the electrostatic energy.

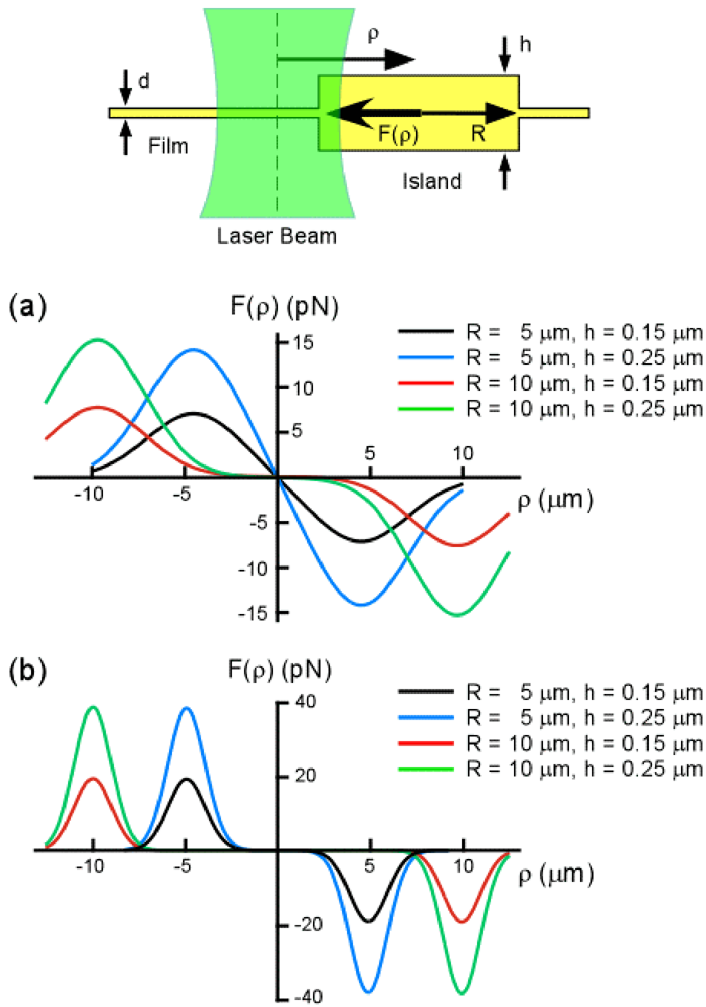


**Figure 6: (a) Radial trapping force F($\rho$), where $\rho$ is the displacement of the island from the center of the beam, computed for various island radii R and thicknesses h, assuming $P$ = 250 mW, $\kappa$ = 2.4, $n$ = 1, $\lambda_0$ = 514.5 nm, $w_0$ = 5 μm, and a film thickness d = 0.05 μm. (b) Trapping force with narrower beam waist ( $w_0$ = 2 μm).**

The calculations also lead to the following conclusions: (1) For a given island radius, the radial trapping force increases with island thickness. (2) For a fixed island thickness, the trapping force is somewhat larger for bigger islands. (3) When the beam waist is small compared to the island radius (for example, with $w_0$ = 2 μm and R = 10 μm, see Fig. 6b), the trapping force is negligible until the edge of the island approaches the beam center. (4) The smaller the beam waist ($w_0$), the higher the optical field gradient and the bigger the maximum trapping force.

### *2. Experimental Determination of Optical Trapping Force*

We have experimentally estimated the degree to which islands in films are trapped by balancing the optical trapping forces against viscous drag. Once an island is trapped, the film can be transported laterally relative to the laser beam by moving the microscope stage at constant speed. The island remains trapped unless the film speed exceeds a critical value, where the viscous drag of the film on the island overcomes the optical trapping force.

We may model the trapped island as a rigid right cylinder extending through the thickness of the film, with its rotational symmetry axis perpendicular to the film plane. If we neglect any interactions with the surrounding air, the drag force on such a stationary cylinder embedded in a flowing isotropic film is given by

$$F_d = \frac{4\pi\eta d v}{\log(R_f / R) - 0.5} \tag{2}$$

where $\eta$ is the viscosity and $d$ the thickness of the film, $v$ is the flow speed of the film, $R_f$ is the radius of the film, and $R$ the radius of the cylinder [10]. In a particular experiment, with $R$ = 10 µm and $R_f$ = 3 mm, we measured a critical speed $v$ = 0.02 mm/s. If we take $\eta$ = 100 poise = 10 kg/m/s and $d$ = 0.05 µm, Eq. (2) yields a critical drag force $F_d$ ~ 20 pN, which is in good agreement with the theoretical peak optical trapping force predicted in the previous section.

## IV. Conclusions

We have demonstrated that islands on freely suspended smectic films and bubbles can be trapped and manipulated using optical tweezers. The experimentally measured maximum trapping force was found to agree with theory. Laser tweezers appear to be a promising tool for studying the static and dynamic interactions between smectic layer steps.

## V. Acknowledgment

This work was supported by NASA Grant NAG3-2457.

## VI. References


[1] G. Friedel, Ann. Phys. (Paris) **18**, 273 (1922).

[2] C. Y. Young, R. Pindak, N. A. Clark, and R. B. Meyer, Phys. Rev. Lett. **40**, 773 (1978).

[3] D. R. Link and N. A. Clark, oral presentation at the Third NASA Microgravity Fluid Physics Conference, Cleveland, OH (1996).

[4] R. Stannarius and C. Cramer, Europhys. Lett. **42**, 43 (1998).

[5] H. Schuring, C. Thieme, and R. Stannarius, Liq. Cryst. **28**, 241 (2001).

[6] J. Li, R. Stannarius, C. Tolksdorf, and R. Zentel, Phys. Chem. Chem. Phys. **5**, 916 (2003).

[7] R. C. Gauthier, J. Opt. Soc. Am. B. **14**, 3323 (1997).

[8] E. Higurashi, O. Ohguchi, and H. Ukita, Opt. Lett. **20**, 1931 (1995).

[9] P. Oswald, P. Pieranski, F. Picano, and R. Holyst, Phys. Rev. Lett. **88**, 015503 (2002).

[10] P. Saffman, J. Fluid Mech. **73**, 593 (1976).